

## Article

# Biomass Allocation, Root Spatial Distribution, and the Physiological Response of *Dalbergia odorifera* Seedlings in Simulated Shallow Karst Fissure-Soil Conditions

Shuzhong Yu , Zhouyou Ni and Zhende Yang \*

Guangxi Key Laboratory of Forest Ecology and Conservation, College of Forestry, Guangxi University, Nanning 530004, China

\* Correspondence: yushuzhong@gxu.edu.cn (S.Y.); dzyang68@gxu.edu.cn (Z.Y.)

**Abstract:** Karst rocky desertification (KRD) is a typical fragile ecological environment with its key and difficult management point being vegetation restoration. Therefore, it is crucial to determine the adaptation mechanisms of suitable plants for ecological restoration in KRD areas. *D. odorifera* is a tall leguminous, woody plant with high medicinal and wood value. This study aimed to explore the adaptation strategy of the *D. odorifera* root system to the shallow karst fissure-soil (SKF-S) habitats. The growth, biomass, spatial root distribution, morphological characteristics, and physiological responses of *D. odorifera* seedlings under different treatments were studied in pots simulating SKF-S habitats. Through the experiments conducted, the following conclusions were obtained: (I) *D. odorifera* enhanced its ability to acquire limited resources through an allocation adjustment strategy (adjusting the biomass allocation strategy, increasing the root shoot ratio, prioritizing organ leaves and 3-level roots), which effectively offset some of the adverse effects; (II) with an increase in the stress severity, *D. odorifera* improved its resource acquisition adaptive strategy by reducing the root diameter and increasing the contact area with soil; (III) the spatial development characteristics of its root system were mainly manifested in the ability to grow vertically, deeper, compared to a horizontal extension; (IV) *D. odorifera* did not passively endure rocky desertification stress but actively improved its metabolism through root metabolic activity and SOD enzyme activity.

**Keywords:** *Dalbergia odorifera*; root system; shallow karst fissure-soil (SKF-S); biomass; spatial distribution; karst rocky desertification (KRD)



**Citation:** Yu, S.; Ni, Z.; Yang, Z. Biomass Allocation, Root Spatial Distribution, and the Physiological Response of *Dalbergia odorifera* Seedlings in Simulated Shallow Karst Fissure-Soil Conditions. *Sustainability* **2022**, *14*, 11348. <https://doi.org/10.3390/su141811348>

Academic Editor: Adriano Sofio

Received: 21 July 2022

Accepted: 7 September 2022

Published: 9 September 2022

**Publisher's Note:** MDPI stays neutral with regard to jurisdictional claims in published maps and institutional affiliations.



**Copyright:** © 2022 by the authors. Licensee MDPI, Basel, Switzerland. This article is an open access article distributed under the terms and conditions of the Creative Commons Attribution (CC BY) license (<https://creativecommons.org/licenses/by/4.0/>).

## 1. Introduction

Karst rocky desertification (KRD) landforms account for 15% of the global land [1] and are typical ecologically fragile areas. Southwest China is one of the three largest KRD areas globally [2]. It is characterized by a large, exposed bedrock area, many rocks and a thin soil layer, high mountains, water scarcity, lack of nutrients, large spatial heterogeneity of the soil, numerous shallow karst fissures (SKFs), soil erosion, difficult water and soil conservation, and severe seasonal and geological structural droughts. Thus, it belongs to a typical fragile ecological environment [3,4] threatening the living environment and economic development of local people and restricting the sustainable development of KRD areas [5,6].

The challenging KRD management point is vegetation restoration [7,8]. To adapt to the local habitat, plants in KRD areas will evolve unique and disparate survival strategies [9,10]. Therefore, it is imperative to determine the adaptation mechanism of suitable plants in such areas for KRD control. For example, the plants' leaves are small and thick and their waxy cuticle is thick [11]. The leaf tissue and vein density are high [12]. Moreover, anti-embolism adaptations can better maintain the photosynthetic efficiency [13]. In severe drought stress, the branches are preferentially protected rather than the leaves [14]. Moreover, the accumulation of proline and soluble sugar is increased to regulate the osmotic potential [11].

Certain plants use  $\text{Ca}^{2+}$  in the habitat to alleviate drought stress [4] since they allocate more biomass to roots [15], while during the dry season, fog water is highly utilized [16,17].

The plant root system is the link between the aboveground and underground ecosystems. It is the key organ for plant physical anchoring, absorption, synthesis, operation, and storage of resources [18], the organ that first feels the changes in the soil environment and is one of the critical factors for improving plant survival rate under stress [19–21]. The growth and development of the plant root system result from the joint action of genetics and the environment [22]. Under different habitat conditions, the morphology, anatomical structure, and physiology of plants of intraspecies often show apparent differentiation [23–25]. In contrast, under uniform habitat conditions, interspecific plants tend to converge [26]. The complexity of the root growth environment and the limitations of root quantitative analysis methods limit the study of the root system [27,28]. Thus far, there has been limited research on the root adaptability of tall arbor species to the soil environment of KRD. This is critical, as tall arbors play a crucial role in maintaining the human living environment in KRD areas.

There are many SKFs in KRD areas [5]. The water runoff will drive the surface soil to fill some SKFs, making them an important means of leakage and unique soil and water storage space [29]. The infertile and thin KRD soil, along with the insufficient water, nutrients, root growth, and plant development space from the surface soil, are the limiting factors for vegetation restoration [30–32]. Shallow karst fissure-soil (SKF-S) is one of the main habitats of plant roots [33], with vital ecological benefits [34], and is one of the key scientific areas of focus for understanding the adaptive mechanism of KRD plants. A study found that plants in KRD areas grow well in a habitat with SKF-S [35], which may be due to adequate water and nutrient storage in SKF-S [36]. This is considered one of the key factors for plant adaptation to karst stress in KRD areas in Southwest China [37,38]. However, as the traditional excavation of the soil profile and micro in situ observations are difficult, there is still a lack of research on how plant roots, especially woody plant roots, adapt to the SKF-S habitats.

*Dalbergia odorifera* T. Chen (*D. odorifera*) is a tall leguminous, woody plant that can fixate nitrogen and improve soil quality. It has high medicinal and timber values. Heartwood of *D. odorifera* is most precious among the 29 species of mahogany in China GB/T18107-2017. It is also a valuable traditional Chinese medicine known as “Jiangxiang”. It has antioxidant, cardiovascular protection, anti-thrombotic platelet aggregation, anti-inflammatory, anti-allergic, central nervous system inhibition, anti-tumor, antibacterial, hypoglycemic, tyrosinase activation, prevention of photoaging, inhibition of osteoclast formation, anti-osteoporosis, and other pharmacological effects [39–41]. *D. odorifera* is suitable for KRD areas, with high average annual net productivity [42]. As reported by Zhou et al. [43], it can improve the soil nutrient status and increase the soil phosphorus availability in KRD areas. Here, we studied the potted seedlings of *D. odorifera* under simulated SKF-S habitats. We performed a comparative analysis of growth, biomass allocation, spatial root distribution, morphological characteristics, and physiology under these conditions. The adaptive response of the *D. odorifera* root system to the SKF-S habitat was further elucidated. Our findings can provide more reasonable strategies and references for ecological restoration in KRD areas.

## 2. Materials and Methods

### 2.1. Plant Materials and Experimental Design

The experiment was conducted in the teaching and scientific research practice base (22°48' N, 108°22' E) of the Forestry College of Guangxi University in Nanning, Guangxi Zhuang Autonomous Region. The region has a typical subtropical monsoon climate, with a long summer and short winter. There are distinct dry and wet seasons, with an annual average rainfall of 1300 mm, precipitation from April to September accounting for 80% of the whole year, and an average yearly temperature of about 21.6 °C, with the highest temperatures observed in July and August.

- (1) Substrate preparation for layered culture

The layered simulation column (defined as type I, Figure 1A) was used to simulate a rocky desertification type in which the surface layer was loam, and the bottom layer was limestone SKFs. The lower layer of the simulation column was a limestone gravel granular layer with variable gravel layer thicknesses of 0 cm, 5 cm, 10 cm, 15 cm, and 20 cm.

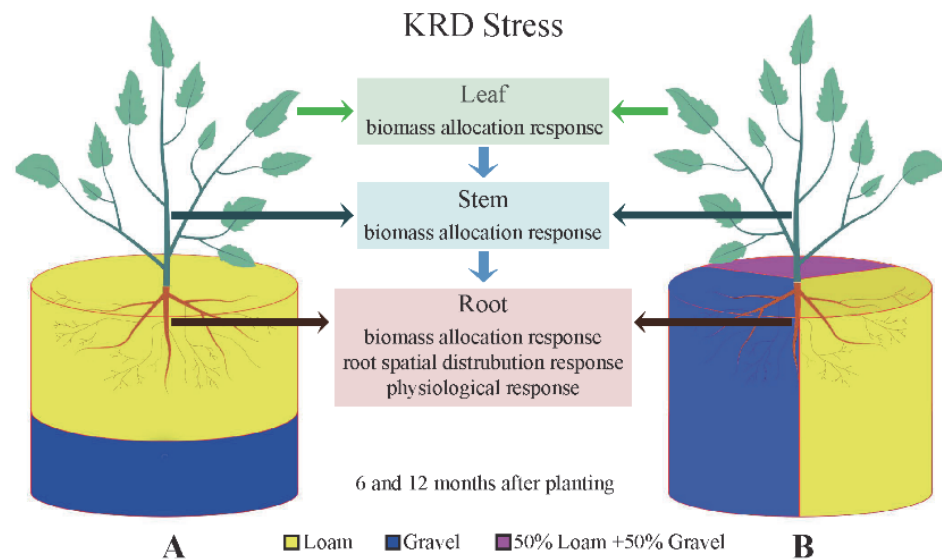


**Figure 1.** Schematic diagram of simulated rocky desertification types I (A) and II (B).

## (2) Preparation of the fan-shaped culture substrate

The fan-shaped simulation column (defined as type II, Figure 1B) was used to simulate a rocky desertification type in which the SKFs of karst limestone fill the loam. The source of the materials and the treatment method were the same as the layered cultivation matrix above. The gravel and loam were prepared into three substrates containing gravel at a 0%, 50%, and 100% volume ratio (Table 1). They were placed in the simulation column at a fan angle of 120° with *D. odorifera* seedlings planted in the middle.

**Table 1.** Soil physical and chemical properties of *D. odorifera*.

Media	pH	Moisture (%)	Total Nitrogen (g·kg <sup>-1</sup> )	Available Phosphorus (mg·kg <sup>-1</sup> )	Available Potassium (mg·kg <sup>-1</sup> )
100% Loam	6.23	33.50	2.18	3.72	55.33
50% Loam + 50% Gravel	8.16	4.17	1.10	5.17	60.67
100% Gravel	9.41	0.56	0.11	0.14	6.43

Note: The data in the table are the mean values.

The loam matrix was collected from the red earth in the rocky desertification area of Mashan County, Guangxi (23°24′–24°2′ N, 107°41′–108°29′ E). The limestone was collected at the same place as the loam soil. After cleaning, the limestone was processed and crushed into ~0.5 cm<sup>3</sup> gravel particles.

One-year-old *D. odorifera* seedlings with uniform growth were used (54–56 cm in height and 0.7–0.9 cm in diameter). They were planted, respectively, in 100% loam (control group, CK), 15 cm topsoil thickness (treatment group 1, T1), 10 cm topsoil thickness (treatment group 2, T2), 5 cm topsoil thickness (treatment group 3, T3), 100% gravel (treatment group 4, T4) and fan-shaped culture substrate (treatment group 5, T5) (Table 2). A total of 15 plants were planted in each treatment group. The cultivation was carried out in a plastic cultivation container (25 cm height × 30 cm width). To facilitate drainage, 2 cm holes were drilled at the bottom of the container. Taking into account the local climatic

conditions, to ensure the seedlings' survival and normal growth at the initial stage of planting, drip irrigation of roots was carried out for 5 min in 5-h intervals. After 30 days, drip irrigation was conducted only once in the morning and in the evening for 5 min. Consistent field management was adopted during the experiment to remove weeds in the container without artificial fertilization regularly. The seedlings' growth and other measurements were performed 12 months after planting.

**Table 2.** The processing groups in different simulated SKF-S.

Media	Groups					T5
	CK	T1	T2	T3	T4	
Gravel layer (cm)	0	5	10	15	20	The fan-shaped simulation column
Loam layer (cm)	20	15	10	5	0	

### 2.2. Determination of the Plant Growth Index

The root length and diameter of *D. odorifera* seedlings were measured with tape and vernier caliper 6 and 12 months after planting. At the 12-month mark, the organs of 18 *D. odorifera* plants were separated. The roots were classified as grade 1, grade 2, and grade 3. The root directly connected with the plant's main stem was labeled as a grade 1 root, the root developed from a grade 1 root was labeled as a grade 2 root, while the root grown from a grade 2 root was labeled as a grade 3 root. Roots were washed with tap and distilled water and were dried with clean paper to measure the fresh weight with an electronic balance. To measure dry weight, the roots, stems, and leaves were placed at 105 °C for 30 min and then dried at 80 °C to a constant weight, which was then recorded.

### 2.3. Determination of Root Morphology and Root Weight Density

(1) The improved whole root excavation method was adopted. The excavation was carried out in four vertical levels: 0–5 cm, 5–10 cm, 10–15 cm, and 15–20 cm, and three horizontal levels: 0–5 cm, 5–10 cm, and 10–15 cm. To ensure that the root system would not be damaged as much when removed from the soil, after digging out the soil with the tools, we manually removed the soil around the root system. The bare root system was cut off after labeling. The soil layers were separated into bags, the collected root system samples were washed in the laboratory, and water on the root surface was removed with absorbent paper. The root system was divided into four grades according to the standards of  $d < 0.5$  mm,  $0.5$  mm  $\leq d < 1$  mm,  $1$  mm  $\leq d < 3$  mm, and  $d \geq 3$  mm. Root morphological data, including root length, root surface area, and root tip number, were obtained by the root analysis system (WinRhizo, Regent Instruments, Quebec, QC, Canada).

(2) Calculation of the horizontal distribution characteristics of root weight density

Calculation formula:

$$\rho = M/\pi(R - R')^2H$$

where  $\rho$  is the root weight density, unit: g/m<sup>3</sup>;  $\pi$  is the PI;  $R$  is the radius of the pot container;  $R'$  is the distance from the trunk;  $H$  is the height of the cultivation substrate 20 cm;  $M$  is the root weight collected in groups.

(3) Calculation of the vertical distribution characteristics of root weight density

Calculation formula:

$$\rho = M/\pi R^2 H'$$

where  $\rho$  is the root weight density, unit: g/m<sup>3</sup>;  $\pi$  is the PI;  $R$  is the radius of the pot container;  $H'$  = layer thickness 5 cm;  $M$  is the root weight collected in groups.

### 2.4. Determination of Plant Physiological Indexes

The activity of peroxidase (POD) and superoxide dismutase (SOD), the content of soluble proteins and soluble sugars, and the root activity were determined. In short, the concentrations of superoxide dismutase (SOD) and peroxidase (POD) were determined according

to the method of Sofo et al. [44]. The soluble protein content was determined according to the Bradford method described by Luo et al. [45]. The soluble carbohydrate content was determined according to the anthrone method described by Yemm and Willis [46]. Root activity was determined according to the method described by Zhang et al. [47].

### 2.5. Statistical Analysis

Microsoft Excel was used for data processing and drawing. SPSS 21.0 was used for the statistical analyses. All values were expressed as mean + SD (standard deviation). One-way analysis of variance (ANOVA) and Duncan multiple range tests were used to test the statistically significant differences between the means.  $p < 0.05$  was considered a significant difference.

## 3. Results

### 3.1. *D. odorifera* Plant Height and Ground Diameter Response to Different SKF-S Conditions

After 6 and 12 months of normal growth of *D. odorifera* in different simulated SKF-S conditions, the plant height increases in T2 were the highest, 1.947 and 1.893 times, respectively (Table 3). The CK exhibited the most significant increase in ground diameter, 2.395 and 3.081-fold, respectively. The plant height after 12 months was lower compared to 6 months because the top branches of *D. odorifera* wither and fall when the temperature is low during the winter.

**Table 3.** *D. odorifera* growth in different simulated SKF-S.

Processing Group	6 Months Later		12 Months Later	
	Plant Height Relative Growth	Ground Diameter Relative Growth	Plant Height Relative Growth	Ground Diameter Relative Growth
CK	1.735 ± 0.058 a	2.359 ± 0.133 a	1.618 ± 0.063 a	3.081 ± 0.091 a
T1	1.687 ± 0.093 a	1.927 ± 0.056 b	1.689 ± 0.047 a	2.536 ± 0.081 b
T2	1.823 ± 0.075 a	1.980 ± 0.051 b	1.755 ± 0.117 a	2.593 ± 0.106 b
T3	1.779 ± 0.064 a	1.964 ± 0.045 b	1.659 ± 0.083 a	2.485 ± 0.125 b
T4	0.899 ± 0.071 b	0.886 ± 0.032 c	0.747 ± 0.039 b	1.586 ± 0.049 c
T5	1.744 ± 0.077 a	2.157 ± 0.124 a	1.657 ± 0.043 a	2.947 ± 0.076 a

Note: Values in the table = mean ± SD. Different letters represent significant difference ( $p < 0.05$ ) between each group.

The plant height increases in all groups, except for T4, showed no significant difference compared to the CK. Significant differences were observed in the growth of ground diameter between the treatment group and the control group. In the treatment group, there was no significant difference between T1, T2, and T3 in terms of plant height and ground diameter growth, all of which were significantly greater compared to T4.

### 3.2. *D. odorifera* Biomass Allocation Response to Different SKF-S Conditions

As shown in Table 4, except for T4, there was no significant difference between the biomass of grade 1 roots in the simulated SKF-S conditions and the CK. Significant differences were observed in the dry weight of the first-order roots in T4 and the first-order roots in other soil conditions. There were significant differences in the dry weight of *D. odorifera* second-order roots between T4 and all the other simulated rocky desertification soil conditions. In T3, the root dry weight of grade 2 was significantly different compared to T2 and T5. No significant differences were observed between the CK and T1, T2, and T5. In T2, the grade 3 root biomass was significantly different compared to CK, T1, T3, and T4, but not compared to T5. There was no significant difference in the dry weight of grade 3 roots between T3 and T4, but there were significant differences between CK and T1, T2, and T5. Finally, there were significant differences in the third-grade root biomass of all simulated SKF-S conditions, except between T5 and T2.

**Table 4.** *D. odorifera* biomass in different simulated SKF-S.

Part	Groups					
	CK	T1	T2	T3	T4	T5
Leaf (g)	119.62 ± 5.74 a	97.63 ± 4.11 ab	118.59 ± 13.89 a	75.83 ± 3.62 b	49.43 ± 1.60 c	108.16 ± 4.52 a
Stem (g)	230.15 ± 11.53 a	178.15 ± 13.88 ab	214.11 ± 8.22 a	112.96 ± 10.31 b	34.19 ± 4.85 c	218.14 ± 7.58 a
Level 1 Root (g)	40.71 ± 2.68 a	30.39 ± 1.67 b	34.51 ± 1.23 ab	14.83 ± 1.02 c	14.83 ± 1.72 c	41.42 ± 1.78 a
Level 2 Root (g)	19.44 ± 1.33 ab	20.99 ± 1.12 ab	24.09 ± 3.19 a	12.93 ± 1.17 b	5.51 ± 0.32 c	24.92 ± 1.45 a
Level 3 Root (g)	29.73 ± 2.04 b	29.42 ± 1.75 b	39.55 ± 2.90 a	35.74 ± 4.92 a	12.69 ± 0.77 c	31.64 ± 2.91 ab
Total Biomass (g)	439.65 ± 22.91 a	356.58 ± 18.97 b	430.85 ± 9.57 a	252.29 ± 7.26 c	116.65 ± 4.00 d	424.28 ± 9.41 a

Note: values in the table = mean ± SD. Different letters represent significant difference ( $p < 0.05$ ) between each group.

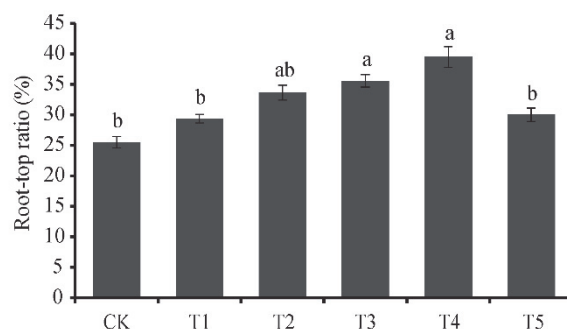
The biomass distribution of *D. odorifera* in different simulated SKF-S conditions was different (Table 5). Except for T5, the biomass distribution of roots, stems, and leaves changed significantly with topsoil thickness reduction, indicating that the biomass distribution ratio of roots and leaves increased gradually with the reduction in topsoil thickness. Stem biomass distribution percentage decreased with the reduction in topsoil thickness. Moreover, root biomass distribution among 1st, 2nd, and 3rd-grade roots changed significantly. With the reduction in topsoil thickness, the percentage of 3rd-grade roots increased gradually, while the proportion of plant biomass allocation to roots and leaves increased. The proportion of root biomass of *D. odorifera* to the third-grade roots increased. Therefore, the different simulated rocky desertification soil conditions affected the biomass allocation of *D. odorifera*.

**Table 5.** *D. odorifera* biomass distribution in different simulated SKF-S.

Part	Groups					
	CK	T1	T2	T3	T4	T5
Leaf (%)	27.21 ± 0.71 b	27.38 ± 0.57 b	27.52 ± 1.10 b	30.06 ± 1.01 b	42.37 ± 1.14 a	25.49 ± 0.52 b
Stem (%)	52.35 ± 1.94 a	49.96 ± 0.78 a	49.69 ± 0.56 a	44.77 ± 0.41 b	29.31 ± 0.64 c	51.41 ± 0.79 a
Level 1 Root (%)	9.26 ± 0.77 a	8.52 ± 0.43 b	8.01 ± 0.50 b	5.88 ± 0.57 c	12.71 ± 0.45 a	9.76 ± 0.36 ab
Level 2 Root (%)	4.42 ± 0.27 a	5.89 ± 0.48 a	5.59 ± 0.27 a	5.13 ± 0.26 a	4.72 ± 0.18 a	5.87 ± 0.22 a
Level 3 Root (%)	6.76 ± 0.19 bc	8.25 ± 0.44 ab	9.18 ± 0.21 a	14.17 ± 0.25 a	10.88 ± 1.19 a	7.46 ± 0.54 b
Total Root Systems (%)	20.44 ± 0.76 b	22.66 ± 0.94 ab	22.78 ± 0.46 ab	25.18 ± 0.73 ab	28.31 ± 1.01 a	23.09 ± 0.42 ab

Note: values in the table = mean ± SD. Different letters represent significant difference ( $p < 0.05$ ) between each group.

The root to shoot ratio of *D. odorifera* reached its maximum in T4, at 39.50%, which was significantly different from the CK, T1, and T5, and not significantly different from the other treatment groups (Figure 2). With the decrease in topsoil thickness, the root to shoot ratio increased gradually.

**Figure 2.** Root-canopy ratio in different simulated SKF-S. Different letters represent significant differences ( $p < 0.05$ ) between each group.

### 3.3. *D. odorifera* Root Spatial Distribution Response to Different SKF-S Conditions

The root weight density of *D. odorifera* in the CK was distributed in different soil layers 0–5 cm away from the trunk, with no significant differences (Figure 3A). It reached its maximum at a soil layer depth of 10 cm, and with the deepening of the soil layer, the root weight density firstly increased and then decreased. At 5–10 cm and 10–15 cm away from the trunk, the same root weight distribution and variation trends were observed in different soil depths.

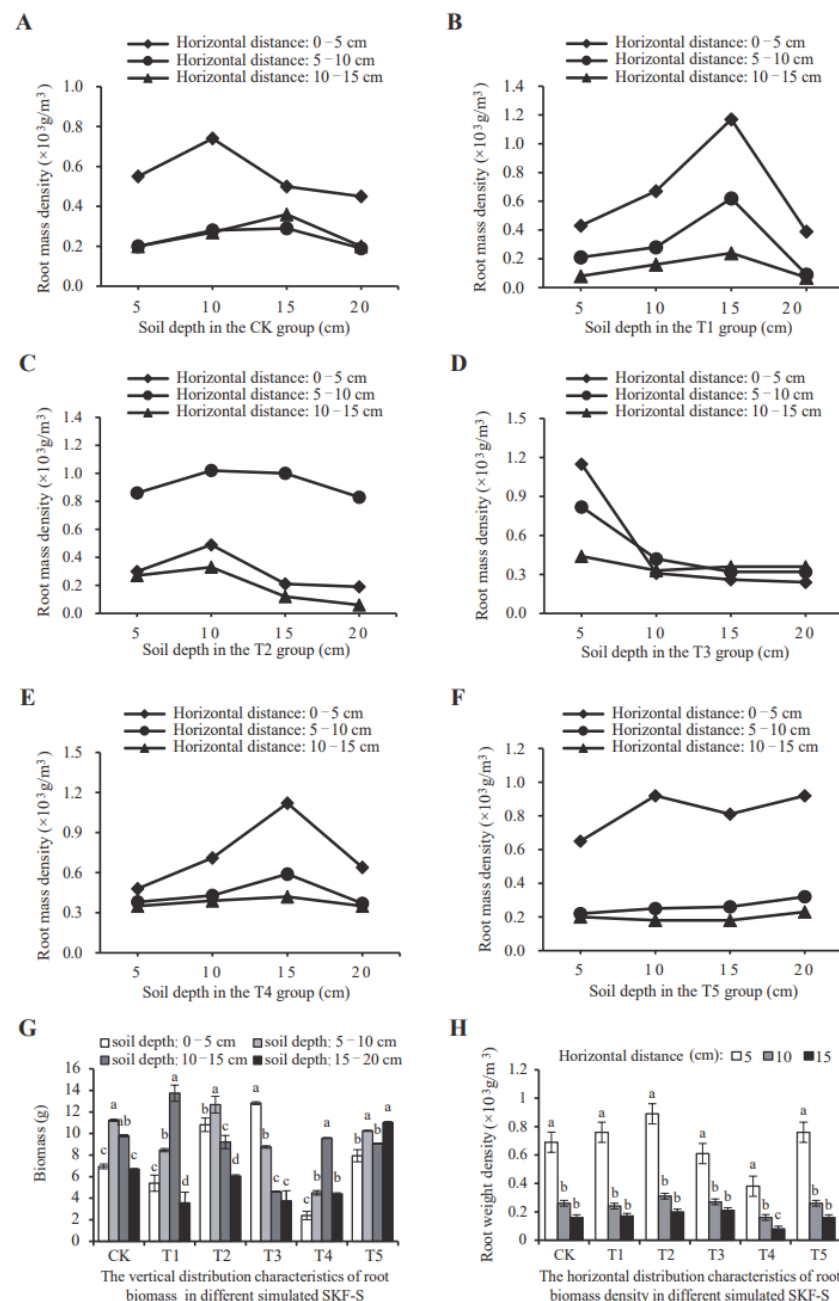


**Figure 3.** Spatial distribution indexes of root weight density in CK (A), T1–T5 (B–F), biomass of *D. odorifera* seedlings in different soil depths in different simulated SKF-S (G), and root weight density at different horizontal distance in different simulated SKF-S (H). Different letters represent significant difference ( $p < 0.05$ ) between different soil depths and horizontal distances in each group.

In T1 (Figure 3B), differences were observed in root weight density distribution in soil layers at different depths. The maximum root weight density at 0–5 cm from the trunk

was observed in the 15 cm soil layer and was significantly different compared to the other soil layers. At a depth of 5–10 cm from the trunk, the root weight density in the 15 cm soil layer was significantly different compared to the other soil layers. However, at a depth of 10–15 cm from the trunk the root system showed no significant differences across soil layers. The root biomass was mainly concentrated in the loam matrix at 0–15 cm and to a lesser extent in the lower layer's gravel layer at 15–20 cm.

In T2 (Figure 3C), differences in the vertical direction were mainly observed at 5–10 cm and 10–15 cm away from the trunk. The root weight density in the 10 cm soil layer was significantly different compared to the 15 cm and 20 cm soil layers. The root system 0–5 cm away from the trunk was evenly distributed in the soil layers of different depths and reached its maximum in the 10 cm soil layer.

In T3 (Figure 3D), the *D. odorifera* root weight density decreased rapidly with soil depth. The root system was mainly distributed in the upper 0–5 cm loam matrix and, to a lesser extent, in the lower 5–20 cm gravel layer. In the 5 cm soil layer, 0–5 cm away from the trunk, the root weight density reached its maximum; however, no significant differences were observed between the soil layers.

In T4 (Figure 3E), the root weight density of *D. odorifera* reached its maximum in the 15 cm soil layer, 0–5 cm away from the trunk, significantly greater than in all other soil layers. Comparing the roots 5–10 cm and 10–15 cm away from the trunk showed a similar trend. In different soil layers, the root weight density 5–10 cm away from the trunk was slightly higher compared to 10–15 cm, albeit with no significant differences. The roots in the 100% gravel soil matrix were mainly concentrated in a 10–20 cm soil layer.

In T5 (Figure 3F) the root weight density in the 10 cm soil layer reached its maximum at a distance of 0–5 cm from the tree trunk. Still, there was no significant difference compared to other soil layers. The distribution and development trend of roots at 5–10 cm and 10–15 cm away from the trunk in the different soil layers were the same. Thus, it can be concluded that *D. odorifera* root biomass was evenly distributed in the vertical direction in the fan-shaped matrix.

The root system of *D. odorifera* had different spatial distribution characteristics under different SKF-S conditions (Figure 3G). In CK, the root biomass first increased and then decreased in the vertical direction along with soil depth. The root biomass was mainly concentrated in the 5–15 cm soil layer. In T1, the distribution of root biomass in each soil layer was significantly different. Root biomass was concentrated in the 5–15 cm soil layer compared to 0–5 cm and 15–20 cm soil layers. In T2, root biomass was mostly concentrated in the 0–15 cm soil layers, with significant differences in biomass distribution observed among different soil layers. In T3, root biomass was concentrated in the 5–10 cm soil layer and was reduced with soil depth. In T4, root biomass was mostly distributed in the 10–15 cm soil layer. In T5, the root biomass increased with soil depth, and the distribution in each soil layer was relatively uniform. Thus, in different simulated rocky desertification soil conditions, root biomass had different distribution characteristics at different depths.

The trend of root weight density of *D. odorifera* decreased with the increase in distance (Figure 3H). There were significant differences between the roots at 0–5 cm and 5–10 cm and 10–15 cm away from the trunk. The distribution of roots at 5–10 cm was greater compared to 10–15 cm, but the difference was insignificant. Compared with the CK, T2 and T3 were decreased, and T4 exhibited the worst root development.

In the spatial distribution of the *D. odorifera* root system in different simulated SKF-S conditions, the spatial development characteristics mainly indicated that the ability to grow vertically was greater than the ability to extend horizontally. In the vertical direction, there was no significant difference in the CK, T2, and T5, in relation to the root weight density with the deepening of soil thickness. In the horizontal direction, the root weight density reached its maximum at 0–5 cm away from the trunk and decreased with the increase in horizontal distance.

### 3.4. Response of *D. odorifera* Root Morphological Characteristics to Different SKF-S Conditions

Under different simulated SKF-S conditions, the total root surface area and total root length are shown in Tables 6 and 7. There was a significant difference in the percentage of the root system with a diameter  $d < 0.5$  mm. With the decrease in topsoil thickness, the percentage of the root system with a diameter  $d < 0.5$  mm increased, among which T4 reached 80%; however, the percentage of the root system with a diameter of  $0.5 \leq d < 1$  mm was further decreased. In particular, in T4 it was only 11%. Under different simulated SKF-S conditions, the ratio of total surface area to total root length was not fixed. The results showed that the average root diameter decreased with a reduction in the topsoil thickness. The increase in gravel promoted the growth of small-diameter roots to a certain extent, and *D. odorifera* could improve resource acquisition by reducing the root diameter and increasing the contact area with soil. T4 (Figure 4A,B) had a greater effect on root tip morphology than CK (Figure 4C,D). In the process of root digging down, some root tips of T4 were enlarged.

**Table 6.** The surface area of the roots in different simulated SKF-S.

Category	Groups					
	CK	T1	T2	T3	T4	T5
Total Root Surface Area (cm <sup>2</sup> )	1261.21 ± 47.61 b	1253.35 ± 40.30 b	1364.97 ± 53.49 ab	918.7 ± 27.17 c	996.94 ± 33.50 c	1412.22 ± 68.98 a
Root Tip Number	12,655 ± 239.17 ab	12,099 ± 213.19 ab	13,084 ± 255.11 a	9981 ± 117.30 b	7243 ± 109.98 c	13,793 ± 305.26 a

Note: values in the table = mean ± SD. Different letters represent significant difference ( $p < 0.05$ ) between each group.

**Table 7.** Root length in different diameters.

Group	Root Length of Different Diameter Classes (cm)				Total Root Length
	$d < 0.5$ mm	$0.5 \text{ mm} \leq d < 1 \text{ mm}$	$1 \text{ mm} \leq d < 3 \text{ mm}$	$d \geq 3 \text{ mm}$	
CK	381.77 ± 6.98 b (38%)	579.25 ± 14.93 a (57%)	36.78 ± 3.27 bc (4%)	15.60 ± 2.59 b (2%)	1013.4
T1	418.21 ± 10.09 ab (50%)	360.27 ± 14.0 b (44%)	30.15 ± 1.55 bc (4%)	14.14 ± 1.29 bc (2%)	822.77
T2	486.28 ± 7.62 a (69%)	164.16 ± 7.17 c (23%)	45.92 ± 3.31 b (7%)	24.73 ± 1.17 a (4%)	703.09
T3	365.76 ± 4.77 b (75%)	63.11 ± 3.29 d (13%)	61.60 ± 3.36 a (13%)	25.69 ± 2.72 a (5%)	489.16
T4	227.41 ± 5.21 c (80%)	39.46 ± 1.52 e (11%)	16.84 ± 1.73 c (5%)	11.54 ± 1.43 c (3%)	345.25
T5	465.16 ± 6.96 ab (64%)	212.89 ± 2.19 c (29%)	33.63 ± 3.07 bc (5%)	13.84 ± 0.30 bc (2%)	725.52

Note: values in the table = mean ± SD. Different letters represent significant difference ( $p < 0.05$ ) between each group.

### 3.5. Response of *D. odorifera* Root System Physiological Indexes to Different SKF-S Conditions

With the decrease in topsoil thickness, the root activity gradually increased. The root activity of *D. odorifera* in the gravel matrix of T4 was the highest, while that of CK was the lowest (Figure 5). With the decrease in topsoil thickness, the root system content of soluble sugars and soluble proteins decreased. Different simulated SKF-S conditions had little effect on root system POD enzyme activity but had a more significant impact on the SOD enzyme activity. With the decrease in topsoil thickness, SOD enzyme activity showed an increasing trend, with T4 exhibiting 164% higher activity compared to the CK (Table 8).

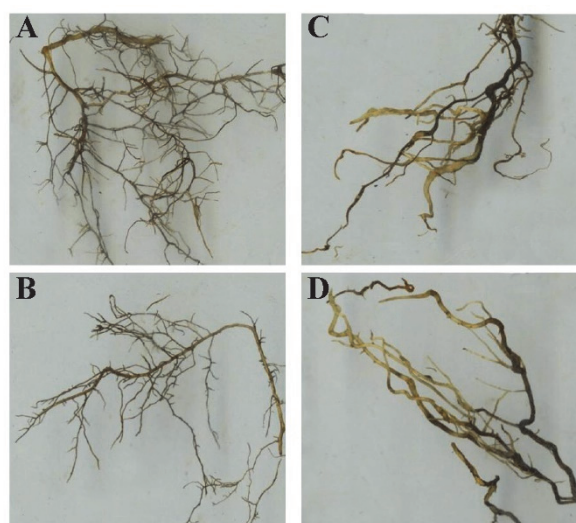


**Figure 4.** Root tip morphology in CK (A,B) and T4 (C,D) of *D. odorifera*.

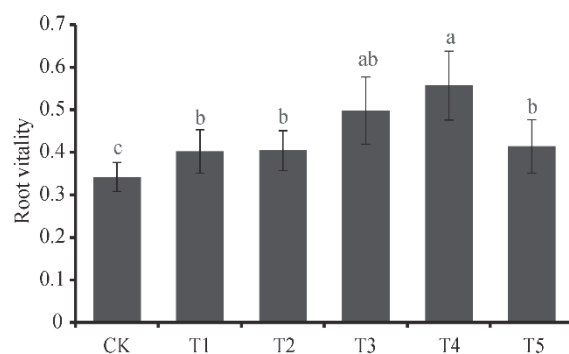


**Figure 5.** The root vitality in different in different simulated SKF-S. Different letters represent significant difference ( $p < 0.05$ ) between each group.

**Table 8.** The contents of soluble sugar and protein, and the activities of SOD and POD in different simulated SKF-S.

Category	Groups					
	CK	T1	T2	T3	T4	T5
Soluble sugar ( $\text{mg}\cdot\text{g}^{-1}$ )	$61.28 \pm 5.33$ a	$55.42 \pm 4.69$ ab	$53.45 \pm 4.28$ b	$36.48 \pm 5.03$ c	$32.29 \pm 2.83$ c	$42.07 \pm 5.14$ bc
Soluble protein ( $\text{mg}\cdot\text{g}^{-1}$ )	$65.32 \pm 4.23$ a	$57.5 \pm 3.35$ b	$44.3 \pm 2.51$ c	$33.3 \pm 2.69$ d	$17.6 \pm 0.29$ e	$43.53 \pm 2.51$ c
SOD ( $\text{U}\cdot\text{g}^{-1}$ )	$182.23 \pm 7.73$ c	$205.93 \pm 4.24$ bc	$212.47 \pm 3.93$ bc	$225.68 \pm 3.73$ b	$299.61 \pm 4.59$ a	$231.14 \pm 3.26$ b
POD ( $\text{U}\cdot\text{g}^{-1}$ )	$380.62 \pm 5.07$ a	$357.18 \pm 7.55$ a	$383.33 \pm 12.26$ a	$351.27 \pm 10.21$ a	$362.10 \pm 4.03$ a	$350.42 \pm 15.41$ a

Note: values in the table = mean  $\pm$  SD. Different letters represent significant difference ( $p < 0.05$ ) between each group.

#### 4. Discussion

##### 4.1. Response of *D. odorifera* Root Growth and Biomass Allocation to Different Simulated SKF-S Conditions

Resource availability changes significantly contribute to the allocation and coordination processes among plant organs [48]. Similarly, it is mainly the adjustment of above-ground parts of light capture driven plants [48,49]. In contrast, the modifications of underground parts are primarily driven by nutrients and water [50]. In this study, the light resources were considered identical. The nutrient and water holding capacity of limestone gravel in each treatment were significantly lower compared to loam. Under limited nutrient

and water conditions, the reduction in plant biomass will negatively affect the growth and development of various organs. However, according to the optimal allocation theory [51], plants usually improve their ability to obtain such limited resources through allocation adjustment strategies to effectively offset some of the adverse effects. Our results showed that the *D. odorifera* root to shoot ratio increased significantly with a decrease in the topsoil thickness. The larger the root shoot ratio, the more beneficial it is for trees to maintain the balance of nutrients and water and survive under severely adverse conditions. This is supported by research results confirming that increasing the distribution of root biomass is crucial for species under nutrient and water stress [49]. With the decrease in topsoil thickness, the biomass distribution of *D. odorifera* roots, stems, and leaves was significantly altered, with the percentage of root and leaf biomass gradually increasing with the decrease in topsoil thickness. In contrast, the percentage of stem biomass decreased. Among them, the percentage of root biomass among all levels of roots also changed significantly: with the decrease in topsoil thickness, the percentage of level 3 roots gradually increased. Thus, our results showed that *D. odorifera* could improve its adaptability to the SKF-S habitat by adjusting its biomass allocation strategy, increasing the root to shoot ratio, and prioritizing investment in organ leaves and third-order roots.

#### 4.2. Response of *D. odorifera* Root System Spatial Distribution to Different Simulated SKF-S Conditions

The spatial structure and distribution of plant roots in the soil determine the amount of soil resources to be explored and obtained. It directly reflects the competitiveness of individual plants or populations to soil resources and is one of the critical characteristics of plant adaptability. In rocky desertification soil, the growth space of plant roots is usually insufficient. According to previous research, the heterogeneity of spatial root distribution is mainly caused by the heterogeneity of soil spatial structure [52]. Through the study on the distribution characteristics of *D. odorifera* root weight density in the soil layer under different simulated SKF-S conditions, we showed that in the vertical direction, there were no significant differences in the CK, T2, and T5 of root weight density with increased soil layer thickness. However, significant differences were observed in root weight density distribution of T1 and T3. The root weight density of T1 initially increased and then was reduced with soil depth. In the 10–15 cm soil layer, the root weight density was significantly higher compared to other layers, whereas in the 15–20 cm soil layer, the root weight density was the lowest. In T3, the root weight density was mainly distributed in the loam layer at a depth of 0–5 cm, while in the gravel layer, the root weight density reached its maximum at a depth of 5–20 cm, which shows a sharp decreasing trend with the increase in depth. Such variability in the distribution of root weight density in these two soil conditions can reflect the plasticity of *D. odorifera* to find a favorable living environment under different soil conditions and compositions. Considering T2 and T5 vertical distribution characteristics of root density, too high or too low gravel thickness will affect the spatial distribution pattern of roots in the soil layer; therefore, the roots will concentrate their development in the loam layer with more abundant resources. In contrast, gravel thickness will not greatly impact the vertical distribution of roots.

Due to the severe seasonal and geological structural drought, the degree of the root system development and the ability to grow the roots vertically is crucial for plants to obtain resources and survive in the harsh environment of KRD [53]. Studies have shown that arbors in KRD areas primarily seek water sources deep underground by vertical root growth. Shrubs and vines will increase water use efficiency and reduce transpiration to resist drought [54,55]. The horizontal distribution characteristics of root weight density in different soil conditions showed that the root weight density reached the maximum at the distance of 0–5 cm from the trunk. There was no significant difference in root weight density with the increase in horizontal distance between 5–10 cm and 10–15 cm from the trunk, except for the 10 cm topsoil thickness matrix. The spatial development characteristics of the *D. odorifera* root system mainly illustrate that the ability of vertical growth was

greater than that of horizontal extension. The resources in the soil of KRD area are spatially very heterogeneous. Plant environmental adaptability can help obtain resources and find favorable habitats by adjusting the spatial distribution of roots, to maximize the use of limited resources and reduce the risk of death. *D. odorifera* can better obtain deep soil resources through the ability of the root system to grow vertically, deeper in the soil, to improve the adaptability to the SKF-S habitat.

#### 4.3. Response of *D. odorifera* Root Morphology to Different Simulated SKF-S Conditions

The plant root morphological characteristics are a direct reflection of their growth and development level and adaptation to the external environment. Generally, plants with a higher number of root tips and total surface area have to absorb water and mineral nutrients. The root diameter is the root morphological character closely related to its total surface. It is a major plasticity determinant of root traits that adapt to the environment [56]. It is considered a key feature in describing the strategy of root resource acquisition and preservation [57], which is closely related to root absorption efficiency, root respiration, mycorrhizal colonization, and root life [28]. With the same root mass, the smaller the root diameter, the larger the contact area with the soil, thus improving the resource acquisition capacity [58]. In different simulated SKF-S conditions,  $t$  the total root length of *D. odorifera* decreased rapidly with the reduction in topsoil thickness reduction. The highest total root length values were observed in the CK, while the lowest was observed in the whole gravel matrix, indicating that the growth of *D. odorifera* was inhibited in the latter. On the other hand, the proportion of root system with a diameter  $d < 0.5$  mm showed a rapidly increasing trend, which slowed the decreasing trend of total surface area. Our results showed that the increase in gravel promoted the growth of small-diameter roots to a certain extent. *D. odorifera* could improve resource acquisition and adaptability to SKF-S habitats by reducing the root diameter and increasing the contact area with soil under the same conditions.

#### 4.4. Response of *D. odorifera* Physiology to Different Simulated SKF-S Conditions

With the decrease in topsoil thickness, the soluble sugar content and soluble protein content of *D. odorifera* root decreased significantly as the soil nutrients were reduced. The dry matter accumulation decreased, indicating that the limited root development decreased *D. odorifera* capacity to absorb water and nutrients. To alleviate the adverse effects on plant growth caused by the reduction in water and nutrient absorption, the *D. odorifera* root system could improve its water and nutrient absorption by improving its physiological function. With the increase in gravel percentage, the root activity and SOD enzyme activity of *D. odorifera* gradually increased, reaching their maximum in the whole gravel soil matrix (T4), indicating that *D. odorifera* root system has strong adaptability in different simulated SKF-S conditions, and can still maintain its physiological and biochemical activities on the exposed rock surface. This phenomenon shows that under the adverse conditions of SKF-S habitat restricting root growth, *D. odorifera* is not passively enduring stress but actively regulating its root physiological metabolism processes. Thus, it is actively improving its ability to absorb water and nutrients to enhance its adaptability to the SKF-S habitat.

Our study showed that *D. odorifera* has good aspects of plasticity in allocation, root-spatial distribution, root morphology, and root physiology. *D. odorifera* adapts to the SKF-S habitat by adjusting its biomass allocation strategy, increasing the root to shoot ratio, and prioritizing the growth of leaves and tertiary roots. It specifically adapts its root system by reducing the root system diameter, thereby increasing the contact area with the soil, shifting root system development to grow vertically to reach deeper soil, better obtaining deep soil resources, and improving the root activity and SOD enzyme activity.

## 5. Conclusions

The KRD environment combines a variety of abiotic stress stresses, such as high temperature, drought, high calcium and magnesium, poor other nutrients, and insufficient

root growth space. Root system is the first important part in response to soil stress. Tall trees and shrubs with deep roots play a more important role in maintaining the living environment in KRD. In this study, we elucidated how *D. odorifera* seedlings adapted to the SKF-S environment in terms of biomass allocation, root spatial distribution, root morphology and physiology. The results provide a scientific basis for the further promotion of *D. orifera* in KRD.

**Author Contributions:** S.Y.: writing—original draft, writing—reviewing and editing, data curation, conceptualization. Z.N.: data curation. Z.Y.: conceptualization. All authors have read and agreed to the published version of the manuscript.

**Funding:** This work was supported by the Natural Science Foundation of China (No. 31760058).

**Institutional Review Board Statement:** Not applicable.

**Informed Consent Statement:** Not applicable.

**Data Availability Statement:** Not applicable.

**Acknowledgments:** We thank Kai Yu (Guangxi University & Nanning Current Science Biotechnology Co., Ltd.) for optimizing the figures and editing this manuscript.

**Conflicts of Interest:** The authors declare no conflict of interest.

## References

1. Ford, D.; Williams, P. *Karst Hydrogeology and Geomorphology*, 2nd ed.; John Wiley & Sons Ltd.: Hoboken, NJ, USA, 2007. [\[CrossRef\]](#)
2. Wang, S.-J.; Li, R.-L.; Sun, C.-X.; Zhang, D.-F.; Li, F.-Q.; Zhou, D.-Q.; Xiong, K.-N.; Zhou, Z.-F. How types of carbonate rock assemblages constrain the distribution of karst rocky desertified land in Guizhou Province, PR China: Phenomena and mechanisms. *Land Degrad. Dev.* **2004**, *15*, 123–131. [\[CrossRef\]](#)
3. Li, S.; Ren, H.; Xue, L.; Chang, J.; Yao, X. Influence of bare rocks on surrounding soil moisture in the karst rocky desertification regions under drought conditions. *Catena* **2014**, *116*, 157–162. [\[CrossRef\]](#)
4. Xue, L.; Ren, H.; Long, W.; Leng, X.; Wang, J.; Yao, X.; Li, S. Ecophysiological Responses of *Calcicole Cyclobalanopsis glauca* (Thunb.) Oerst. to Drought Stress and Calcium Supply. *Forests* **2018**, *9*, 667. [\[CrossRef\]](#)
5. Yan, Y.; Dai, Q.; Jin, L.; Wang, X. Geometric morphology and soil properties of shallow karst fissures in an area of karst rocky desertification in SW China. *Catena* **2019**, *174*, 48–58. [\[CrossRef\]](#)
6. Wang, S.-J.; Liu, Q.-M.; Zhang, D.-F. Karst rocky desertification in southwestern China: Geomorphology, landuse, impact and rehabilitation. *Land Degrad. Dev.* **2004**, *15*, 115–121. [\[CrossRef\]](#)
7. Qi, X.; Wang, K.; Zhang, C. Effectiveness of ecological restoration projects in a karst region of southwest China assessed using vegetation succession mapping. *Ecol. Eng.* **2013**, *54*, 245–253. [\[CrossRef\]](#)
8. Li, D.; Zhang, X.; Green, S.M.; Dungait, J.; Wen, X.; Tang, Y.; Guo, Z.; Yang, Y.; Sun, X.; Quine, T.A. Nitrogen functional gene activity in soil profiles under progressive vegetative recovery after abandonment of agriculture at the Puding Karst Critical Zone Observatory, SW China. *Soil Biol. Biochem.* **2018**, *125*, 93–102. [\[CrossRef\]](#)
9. Delzon, S. New insight into leaf drought tolerance. *Funct. Ecol.* **2015**, *29*, 1247–1249. [\[CrossRef\]](#)
10. Zhang, S.; Zhang, Y.; Xiong, K.; Yu, Y.; Min, X. Changes of leaf functional traits in karst rocky desertification ecological environment and the driving factors. *Glob. Ecol. Conserv.* **2020**, *24*, e01381. [\[CrossRef\]](#)
11. Geekiyanage, N.; Goodale, U.M.; Cao, K.-F.; Kitajima, K. Leaf trait variations associated with habitat affinity of tropical karst tree species. *Ecol. Evol.* **2017**, *8*, 286–295. [\[CrossRef\]](#)
12. Qi, D.; Wieneke, X.; Zhou, X.; Jiang, X.; Xue, P. Succession of plant community composition and leaf functional traits in responding to karst rocky desertification in the Wushan County in Chongqing, China. *Community Ecol.* **2017**, *18*, 157–168. [\[CrossRef\]](#)
13. Chen, Y.; Choat, B.; Sterck, F.; Maenpue, P.; Katabuchi, M.; Zhang, S.; Tomlinson, K.W.; Oliveira, R.S.; Zhang, Y.; Shen, J.; et al. Hydraulic prediction of drought-induced plant dieback and top-kill depends on leaf habit and growth form. *Ecol. Lett.* **2021**, *24*, 2350–2363. [\[CrossRef\]](#)
14. Zhang, Q.; Zhu, S.; Jansen, S.; Cao, K. Topography strongly affects drought stress and xylem embolism resistance in woody plants from a karst forest in Southwest China. *Funct. Ecol.* **2021**, *35*, 566–577. [\[CrossRef\]](#)
15. Ni, J.; Luo, D.H.; Xia, J.; Zhang, Z.H.; Hu, G. Vegetation in karst terrain of southwestern China allocates more biomass to roots. *Solid Earth* **2015**, *6*, 799–810. [\[CrossRef\]](#)
16. Wu, Y.; Song, L.; Liu, W.; Liu, W.; Li, S.; Fu, P.; Shen, Y.; Wu, J.; Wang, P.; Chen, Q.; et al. Fog Water Is Important in Maintaining the Water Budgets of Vascular Epiphytes in an Asian Tropical Karst Forests during the Dry Season. *Forests* **2018**, *9*, 260. [\[CrossRef\]](#)
17. Fu, P.-L.; Liu, W.-J.; Fan, Z.-X.; Cao, K.-F. Is fog an important water source for woody plants in an Asian tropical karst forest during the dry season? *Ecology* **2016**, *9*, 964–972. [\[CrossRef\]](#)

18. Bardgett, R.D.; Mommer, L.; De Vries, F.T. Going underground: Root traits as drivers of ecosystem processes. *Trends Ecol. Evol.* **2014**, *29*, 692–699. [[CrossRef](#)]
19. Johnson, D.M.; Domec, J.-C.; Berry, Z.C.; Schwantes, A.; McCulloh, K.A.; Woodruff, D.R.; Polley, H.W.; Wortemann, R.; Swenson, J.J.; Mackay, D.; et al. Co-occurring woody species have diverse hydraulic strategies and mortality rates during an extreme drought. *Plant Cell Environ.* **2018**, *41*, 576–588. [[CrossRef](#)]
20. Crouchet, S.E.; Jensen, J.; Schwartz, B.F.; Schwinning, S. Tree Mortality after a Hot Drought: Distinguishing Density-Dependent and -Independent Drivers and Why It Matters. *Front. For. Glob. Chang.* **2019**, *2*, 21. [[CrossRef](#)]
21. Ding, Y.; Nie, Y.; Chen, H.; Wang, K.; Querejeta, J.I. Water uptake depth is coordinated with leaf water potential, water-use efficiency and drought vulnerability in karst vegetation. *New Phytol.* **2021**, *229*, 1339–1353. [[CrossRef](#)]
22. Arnold, P.A.; Kruuk, L.E.B.; Nicotra, A.B. How to analyse plant phenotypic plasticity in response to a changing climate. *New Phytol.* **2019**, *222*, 1235–1241. [[CrossRef](#)] [[PubMed](#)]
23. Weemstra, M.; Freschet, G.T.; Stokes, A.; Roumet, C. Patterns in intraspecific variation in root traits are species-specific along an elevation gradient. *Funct. Ecol.* **2021**, *35*, 342–356. [[CrossRef](#)]
24. Salmela, M.J. Patterns of genetic diversity vary among shoot and root functional traits in Norway spruce *Picea abies* along a latitudinal gradient. *Oikos* **2021**, *139*, 1143–1157. [[CrossRef](#)]
25. Kumordzi, B.B.; Aubin, I.; Cardou, F.; Shipley, B.; Violle, C.; Johnstone, J.; Anand, M.; Arsenault, A.; Bell, F.W.; Bergeron, Y.; et al. Geographic scale and disturbance influence intraspecific trait variability in leaves and roots of North American understory plants. *Funct. Ecol.* **2019**, *33*, 1771–1784. [[CrossRef](#)]
26. Colom, S.M.; Baucom, R.S. Below-ground competition favors character convergence but not character displacement in root traits. *New Phytol.* **2021**, *229*, 3195–3207. [[CrossRef](#)] [[PubMed](#)]
27. Freschet, G.T.; Pagès, L.; Iversen, C.M.; Comas, L.H.; Rewald, B.; Roumet, C.; Klimešová, J.; Zadworny, M.; Poorter, H.; Postma, J.A.; et al. A starting guide to root ecology: Strengthening ecological concepts and standardising root classification, sampling, processing and trait measurements. *New Phytol.* **2021**, *232*, 973–1122. [[CrossRef](#)]
28. Freschet, G.T.; Roumet, C.; Comas, L.H.; Weemstra, M.; Bengough, A.G.; Rewald, B.; Bardgett, R.D.; De Deyn, G.B.; Johnson, D.; Klimešová, J.; et al. Root traits as drivers of plant and ecosystem functioning: Current understanding, pitfalls and future research needs. *New Phytol.* **2021**, *232*, 1123–1158. [[CrossRef](#)]
29. Huang, W.; Zhong, Y.; Song, X.; Zhang, C.; Ren, M.; Du, Y. Seasonal Differences in Water-Use Sources of *Impatiens hainanensis* (Balsaminaceae), a Limestone-Endemic Plant Based on “Fissure-Soil” Habitat Function. *Sustainability* **2021**, *13*, 8721. [[CrossRef](#)]
30. Chang, J.; Zhu, J.; Xu, L.; Su, H.; Gao, Y.; Cai, X.; Peng, T.; Wen, X.; Zhang, J.; He, N. Rational land-use types in the karst regions of China: Insights from soil organic matter composition and stability. *Catena* **2018**, *160*, 345–353. [[CrossRef](#)]
31. Zhang, X.; Hu, M.; Guo, X.; Yang, H.; Zhang, Z.; Zhang, K. Effects of topographic factors on runoff and soil loss in Southwest China. *Catena* **2018**, *160*, 394–402. [[CrossRef](#)]
32. Liu, Y.; Wei, X.; Zhou, Z.; Shao, C.; Su, S. Influence of Heterogeneous Karst Microhabitats on the Root Foraging Ability of Chinese Windmill Palm (*Trachycarpus fortunei*) Seedlings. *Int. J. Environ. Res. Public Health* **2020**, *17*, 434. [[CrossRef](#)] [[PubMed](#)]
33. Yan, Y.; Dai, Q.; Wang, X.; Jin, L.; Mei, L. Response of shallow karst fissure soil quality to secondary succession in a degraded karst area of southwestern China. *Geoderma* **2019**, *348*, 76–85. [[CrossRef](#)]
34. Wang, J.; Zou, B.; Liu, Y.; Tang, Y.; Zhang, X.; Yang, P. Erosion-creep-collapse mechanism of underground soil loss for the karst rocky desertification in Chenqi village, Puding county, Guizhou, China. *Environ. Earth Sci.* **2014**, *72*, 2751–2764. [[CrossRef](#)]
35. Nie, Y.-P.; Chen, H.-S.; Wang, K.-L.; Tan, W.; Deng, P.-Y.; Yang, J. Seasonal water use patterns of woody species growing on the continuous dolostone outcrops and nearby thin soils in subtropical China. *Plant Soil* **2011**, *341*, 399–412. [[CrossRef](#)]
36. Li, Y.; Liu, Z.; Liu, G.; Xiong, K.; Cai, L. Dynamic variations in soil moisture in an epikarst fissure in the karst rocky desertification area. *J. Hydrol.* **2020**, *591*, 125587. [[CrossRef](#)]
37. Peng, X.; Dai, Q.; Ding, G.; Shi, D.; Li, C. Impact of vegetation restoration on soil properties in near-surface fissures located in karst rocky desertification regions. *Soil Tillage Res.* **2020**, *200*, 104620. [[CrossRef](#)]
38. Yan, Y.; Dai, Q.; Yang, Y.; Yan, L.; Yi, X. Epikarst shallow fissure soil systems are key to eliminating karst drought limitations in the karst rocky desertification area of SW China. *Ecohydrology* **2021**, *15*, e2372. [[CrossRef](#)]
39. Zhao, X.; Wang, C.; Meng, H.; Yu, Z.; Yang, M.; Wei, J. *Dalbergia odorifera*: A review of its traditional uses, phytochemistry, pharmacology, and quality control. *J. Ethnopharmacol.* **2020**, *248*, 112328. [[CrossRef](#)]
40. Wariss, H.M.; Yi, T.-S.; Wang, H.; Zhang, R. Characterization of the complete chloroplast genome of *Dalbergia odorifera* (Leguminosae), a rare and critically endangered legume endemic to China. *Conserv. Genet. Resour.* **2017**, *10*, 527–530. [[CrossRef](#)]
41. Ma, R.K.; Luo, J.; Qiao, M.J.; Fu, Y.L.; Zhu, P.C.; Wei, P.L.; Liu, Z.G. Chemical composition of extracts from *Dalbergia odorifera* heartwood and its correlation with color. *Ind. Crop. Prod.* **2022**, *180*, 114728. [[CrossRef](#)]
42. Li, M.; You, Y.; Tan, X.; Wen, Y.; Yu, S.; Xiao, N.; Shen, W.; Huang, X. Mixture of N<sub>2</sub>-fixing tree species promotes organic phosphorus accumulation and transformation in topsoil aggregates in a degraded karst region of subtropical China. *Geoderma* **2022**, *413*, 115752. [[CrossRef](#)]
43. Zhou, X.G.; Sun, D.J.; Wen, Y.G.; Wang, L.; Ming, A.A.; Jia, H.Y.; Zhu, H.G.; Zhao, Y.Y.; Huang, Y.J.; Liang, J. Biomass, Productivity and Their Dynamic Changes of Different Restoration Stands in Karst Rocky Desertification. *Guangxi Sci.* **2022**, *29*, 98–107. [[CrossRef](#)]

44. Sofo, A.; Dichio, B.; Xiloyannis, C.; Masia, A. Effects of different irradiance levels on some antioxidant enzymes and on malondialdehyde content during rewatering in olive tree. *Plant Sci.* **2004**, *166*, 293–302. [[CrossRef](#)]
45. Luo, Z.-B.; Calfapietra, C.; Scarascia-Mugnozza, G.; Liberloo, M.; Polle, A. Carbon-based secondary metabolites and internal nitrogen pools in *Populus nigra* under Free Air CO<sub>2</sub> Enrichment (FACE) and nitrogen fertilisation. *Plant Soil* **2008**, *304*, 45–57. [[CrossRef](#)]
46. Yemm, E.W.; Willis, A.J. The estimation of carbohydrates in plant extracts by anthrone. *Biochem. J.* **1954**, *57*, 508–514. [[CrossRef](#)]
47. Zhang, Z.L.; Qu, W.J.; Li, X.F. *Experimental Guidance for Plant Physiology*; Higher Education Press: Beijing, China, 2009.
48. Poorter, H.; Jagodzinski, A.; Ruiz-Peinado, R.; Kuyah, S.; Luo, Y.; Oleksyn, J.; Usoltsev, V.A.; Buckley, T.N.; Reich, P.; Sack, L. How does biomass distribution change with size and differ among species? An analysis for 1200 plant species from five continents. *New Phytol.* **2015**, *208*, 736–749. [[CrossRef](#)]
49. Freschet, G.T.; Swart, E.; Cornelissen, J.H.C. Integrated plant phenotypic responses to contrasting above- and below-ground resources: Key roles of specific leaf area and root mass fraction. *New Phytol.* **2015**, *206*, 1247–1260. [[CrossRef](#)]
50. Freschet, G.T.; Violle, C.; Bourget, M.Y.; Scherer-Lorenzen, M.; Fort, F. Allocation, morphology, physiology, architecture: The multiple facets of plant above- and below-ground responses to resource stress. *New Phytol.* **2018**, *219*, 1338–1352. [[CrossRef](#)]
51. Shipley, B.; Meziane, D. The balanced-growth hypothesis and the allometry of leaf and root biomass allocation. *Funct. Ecol.* **2002**, *16*, 326–331. [[CrossRef](#)]
52. Jackson, R.B.; Mooney, H.A.; Schulze, E.-D. A global budget for fine root biomass, surface area, and nutrient contents. *Proc. Natl. Acad. Sci. USA* **1997**, *94*, 7362–7366. [[CrossRef](#)]
53. He, C.X.; Huang, Y.Q.; Li, X.K.; Wang, X.Y.; Wang, Q. The ecophysiological traits of three karst rocky desert restoration species. *Guihaia* **2007**, *27*, 53–61.
54. Ni, L.K.; Gu, D.X.; He, W.; Huang, Y.Q.; Chen, Z.Y. Research advances in plant ecological adaptability in karst area. *Chin. J. Ecol.* **2019**, *38*, 2210–2217. [[CrossRef](#)]
55. Savi, T.; Petruzzellis, F.; Moretti, E.; Stenni, B.; Zini, L.; Martellos, S.; Lisjak, K.; Nardini, A. Grapevine water relations and rooting depth in karstic soils. *Sci. Total Environ.* **2019**, *692*, 669–675. [[CrossRef](#)]
56. Ma, Z.; Guo, D.; Xu, X.; Lu, M.; Bardgett, R.D.; Eissenstat, D.M.; McCormack, M.L.; Hedin, L.O. Evolutionary history resolves global organization of root functional traits. *Nature* **2018**, *555*, 94–97. [[CrossRef](#)]
57. Kong, D.; Wang, J.; Wu, H.; Valverde-Barrantes, O.J.; Wang, R.; Zeng, H.; Kardol, P.; Zhang, H.; Feng, Y. Nonlinearity of root trait relationships and the root economics spectrum. *Nat. Commun.* **2019**, *10*, 2203. [[CrossRef](#)]
58. Abenavoli, M.R.; Leone, M.; Sunseri, F.; Bacchi, M.; Sorgonà, A. Root Phenotyping For Drought Tolerance in Bean Landraces From Calabria (Italy). *J. Agron. Crop Sci.* **2016**, *202*, 1–12. [[CrossRef](#)]